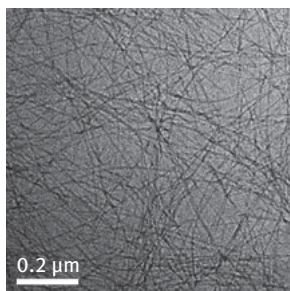


# 5 Organic and biological nanoparticles

The organic and biological worlds have contributed a variety of materials to the “nanoparticle universe”. Some of these nanostructures occur in natural/physiological environments (for example peptide “nanofibers”), and many are synthetic entities, including polymeric NPs or NPs built from organic compounds. For reasons of space and scope, this chapter focuses on biological and organic molecule assemblies which can be categorized as “*synthetic nanoparticles*”; many other fascinating biological, polymer, and organic molecular systems exhibiting nanostructural features cannot be discussed here and the reader is referred to the pertinent literature.

## 5.1 Biological nanoparticles

From proteins to deoxyribonucleic acid (DNA) to lipids, biology provides a plethora of molecules which tend to self-assemble, and as such often produce nanoscale aggregates. Various *biological nanostructures* have been identified in nature, some of which in fact are implicated in devastating diseases, such as amyloid nanofibers, which are among the pathological hallmarks of Alzheimer’s disease (Fig. 5.1). Furthermore, the diverse synthetic and biochemical methods available for modifying and functionalizing biomolecules provide ample means to control the structural outcomes of biological self-assembled nanostructures, creating varied biomimetic nanostructures. This section focuses on aggregates which are more closely defined as “nanoparticles” – entities which conform to the generic classification of stand-alone structures being small, from a few to tens of nanometers.

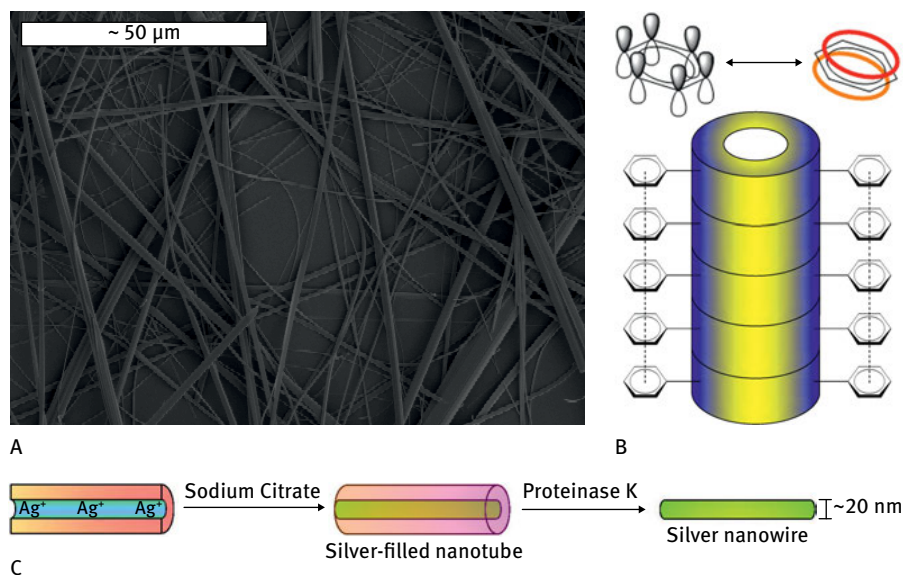


**Fig. 5.1:** Amyloid nanofibers. Electron microscopy image showing long fibers assembled spontaneously by beta-amyloid, the ubiquitous peptide which forms amyloid plaques in the brains of Alzheimer’s disease patients.

*Tubular peptide nanoparticles* (also referred to as “*peptide nanotubes*”) have attracted significant interest from several angles. These fascinating morphologies depend to a large degree on the amino acid sequences of the constituent peptides (and thus can be tuned by modifying the peptide sequence). Furthermore, as these anisotropic NP structures mimic physiologically-encountered tubular and fibrillar peptide aggregates

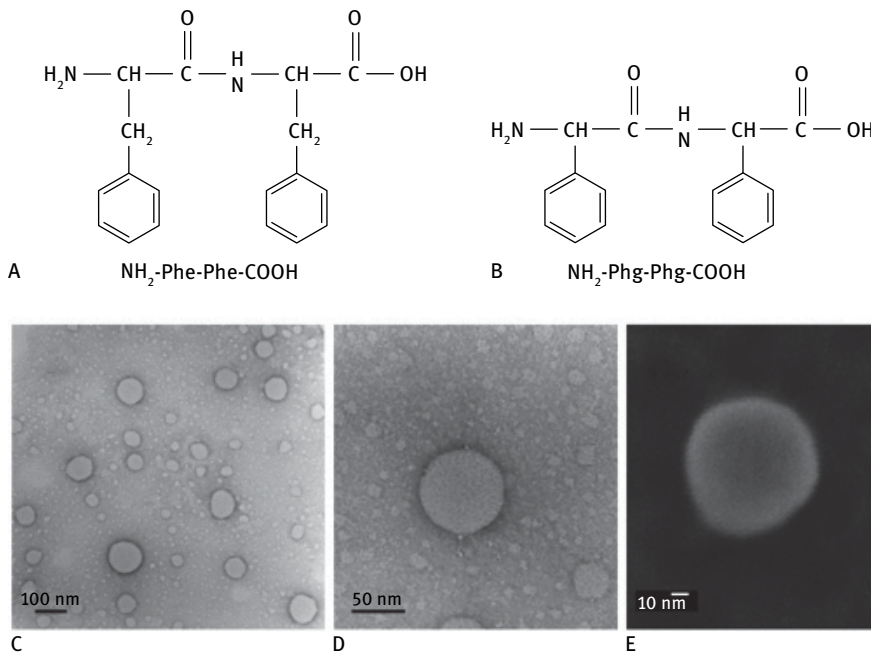
(e.g. the amyloid fibers shown in Fig. 5.1), they could help to better understand the pathologies of diseases such as Alzheimer's. Also important, peptide nanotubes and nanofibers can serve as templates for functional materials – for example as scaffoldings for fabrication of metal nanowires and nanotubes.

Figure 5.2 illustrates the use of a synthetic peptide nanotube as a template for metal nanowire formation. A short dipeptide comprising of two phenylalanine residues (i.e. an “FF” peptide sequence, using the single letter notation for phenylalanine) was shown by E. Gazit and colleagues at Tel Aviv University, Israel, to adopt elongated nanotubular morphology (Fig. 5.2A). Self-assembly of such nanotubes is presumed to occur through interactions between adjacent *aromatic* residues of amino acids such as phenylalanine and tyrosine (i.e. “ $\pi$  stacking”; Fig. 5.2B). The peptide nanotubes were subsequently used as templates to cast metal nanowires through embedding metal (silver) ions within the nanotubes, which generated silver nanowires after reduction (Fig. 5.2C). The peptide nanotube scaffold could be dissolved by simple enzymatic degradation, not requiring harsh conditions or environmentally harmful reagents, underscoring a potential advantage of this “biomimetic” strategy for fabrication of metallic nanowires.



**Fig. 5.2:** Dipeptide nanofibers as templates for metal nanowires. **A:** Electron microscopy image of diphenylalanine (Phe-Phe) nanofibers. Image courtesy of E. Gazit, Tel Aviv University, Israel. **B:** Model of the  $\pi$ -stacking mechanism hypothesized to produce the nanofibers via interactions between the aromatic rings of phenylalanine. **C:** Use of the peptide nanotube as a template for construction of silver nanowires through reduction of  $\text{Ag}^+$  ions embedded inside the tubes.

Short peptide motifs were shown to produce other morphologies. Figure 5.3 depicts intriguing spherical “caged” NPs comprising *diphenylglycine*. While diphenylalanine (which produced elongated nanotubes; Fig. 5.2), it exhibits a more rigid conformation due to the absence of a C-CH<sub>2</sub>-C bond between the backbone and aromatic residues (giving rise to less rotational degrees of freedom; Fig. 5.3B). This structural feature is likely responsible for the formation of spherical NPs. Remarkably, E. Gazit and colleagues at Tel Aviv University, Israel, have shown that the spherical peptide NPs were not degraded even in extreme conditions such as elevated temperatures or highly acidic and basic solutions, pointing to the putative role of  $\pi$ -stacking interactions in nanoparticle stability.



**Fig. 5.3:** Spherical “caged” nanoparticles comprising of diphenylglycine. **A:** Diphenylalanine and **B:** diphenylglycine chemical structures. **C–E:** Electron microscopy images showing spherical diphenylglycine nanoparticles. Reprinted with permission from Reches and Gazit, *Nano Lett.* **4** (2004), 581–585, © 2004 The American Chemical Society.

The dramatic differences in nanoparticle morphologies between the two closely-related dipeptides – nanotubes vs nanospheres (Figures 5.2 and 5.3) – triggered efforts to further exploit the structural variability in order to develop new dipeptide-based NP assembly processes. Figure 5.4 highlights experimental data showing a reversible transformation between diphenylalanine spherical NPs and nanotubes achieved by changing the *solution properties*. Specifically, G. Rosenman and colleagues at Tel

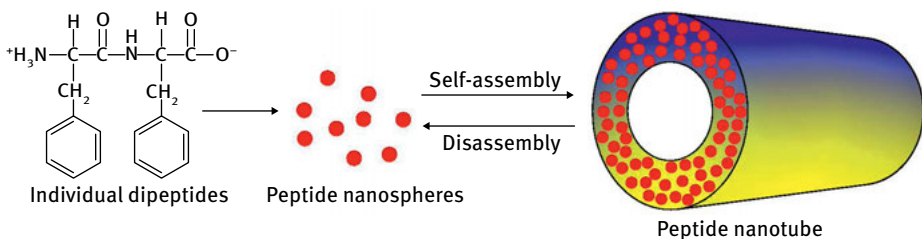


**Fig. 5.4:** Reversible transition between dipptide nanospheres and a nanotube. Diphenylalanines spontaneously assemble into spherical nanoparticles in methanol, while changing the solvent to water induces formation of nanotubes.

Aviv University, Israel, discovered that concentrated solutions of diphenylalanine in methanol produced nanosize spherical NPs (reminiscent of “quantum dots”), while changing the solvent to water initiated self-assembly of the nanospheres into *nanotubes*. This nanosphere-to-nanotube transformation was fully reversible, induced simply by changing the solvent. The researchers hypothesized that the polar organic solvent aided stabilization of the peptide “dots”, while in the aqueous environment the individual NPs made of hydrophobic residues were drawn together, forming nanotubes.

Modulation of the amino acid *sequences* has been the predominant strategy to control peptide self-assembly properties, making formation of nanofibers, nanotubes, and nanospheres with tunable dimensionalities and morphologies possible. Other strategies have added *nonpeptide* components to the biological nanoparticle construction toolbox. Figure 5.5 portrays an anti-tumor peptide covalently bonded to a hydrophobic hydrocarbon moiety. Even though the peptide itself is hydrophilic and dissolves in water, attachment of the lipid-like residue promoted self-assembly of the “peptide amphiphiles” into nanotubular aggregates (which can also be characterized as “micellar assemblies”). Such nanotubes offer distinct advantages as therapeutic vehicles. The tubular structure enables high loading of the biologically-active peptide cargo through condensation, and the amphiphilic layer protects the peptide from enzymatic degradation in physiological environments (e.g. the bloodstream) until it reaches its destination. Furthermore, the hydrophobic coating allows docking of the nanotube onto the cell membrane and subsequent injection of the peptide molecules into the cell. The peptide nanotube could also undergo gradual disintegration enabling slow release of the therapeutic molecules.

Integrating peptides and lipid molecules within composite nanoparticles has been pursued as a promising therapeutic strategy. In addition to covalent binding between peptides and lipids (as in the peptide amphiphile system discussed above), studies have shown that *noncovalent association* can also lead to new NP species exhibiting useful functionalities. Figure 5.6, for example, depicts “core-shell” spherical NPs produced by mixing a therapeutic drug, phospholipids, and a helical peptide.

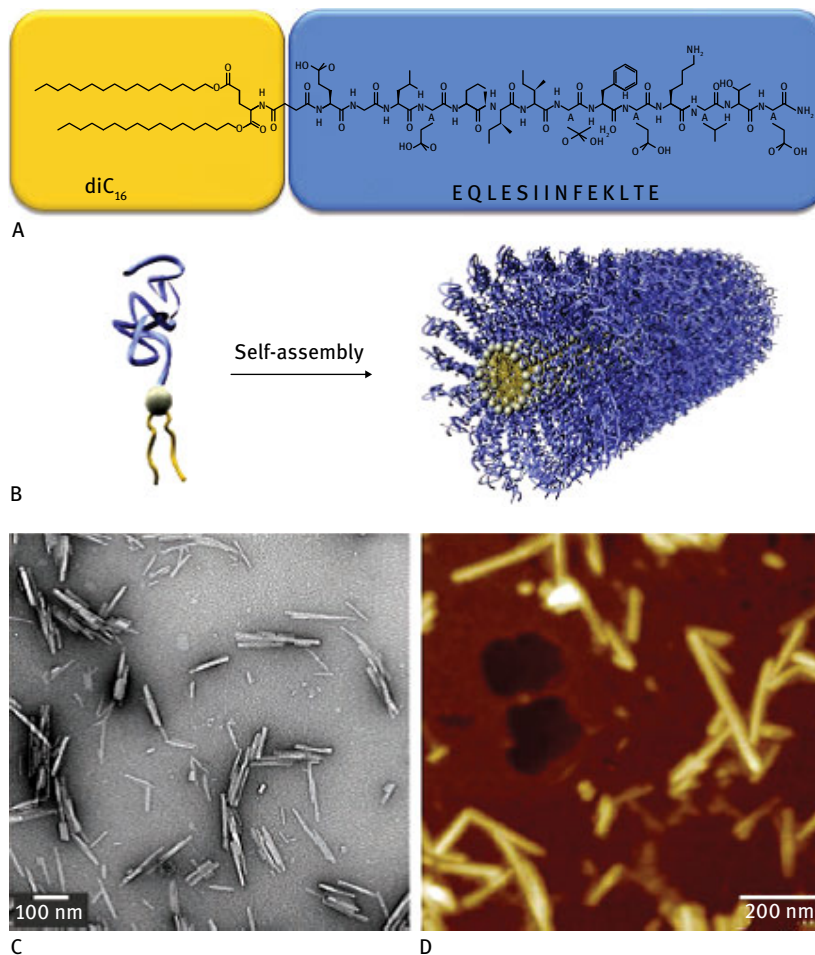


**Fig. 5.5:** Nanotubes assembled from peptide-amphiphiles. **A:** Chemical structure of the peptide amphiphile, comprising of a hydrophobic hydrocarbon chain (yellow background) covalently linked to a short hydrophilic peptide (blue background). **B:** Schematic depiction of nanotube formation through self-assembly of the peptide amphiphiles. **C:** Electron microscopy. **D:** Atomic force microscopy images showing the nanotubes. Reprinted with permission from Black et al., *Adv. Mater.* **24** (2012), 3845–3849, © 2012 John Wiley & Sons.

The objective underlying the choice of molecular composition and overall structure of these NPs was to achieve a delivery system that would both protect the bio-active cargo from degradation prior to reaching its target and also provide the means for delivery into the cell interior. In general, particles made of only phospholipids (i.e. lipid vesicles or liposomes) are not considered effective drug delivery vehicles since they are not stable for extended periods in the bloodstream as they spontaneously disintegrate and/or are degraded by lipophilic enzymes. To overcome this barrier, G. Zheng and

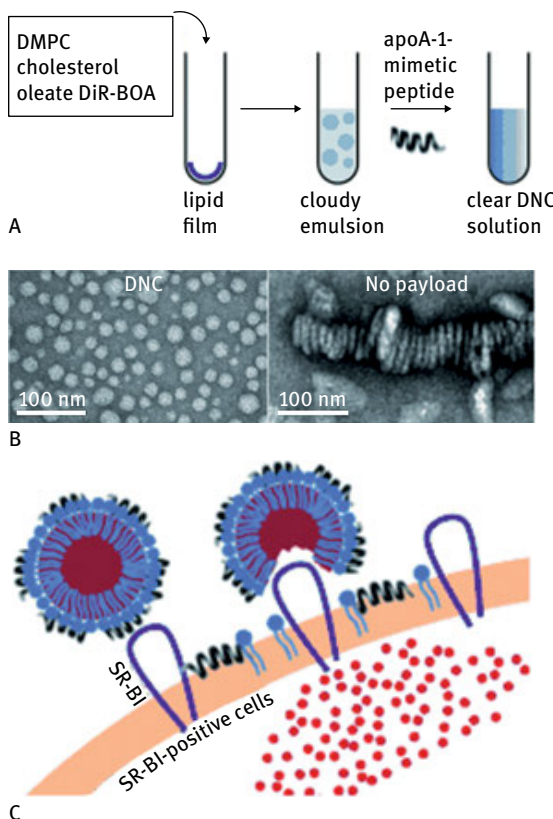


**Fig. 5.6:** Drug nanocarrier (DNC) constructed from a mixture of lipid/peptide/drug. **A:** DNC preparation procedure; noncovalent incorporation of the peptide induces formation of water-soluble nanoparticles, recognized by cell-displayed receptors. **B:** Electron microscopy images showing the compacted DNC nanoparticles (left), and the discoidal structures formed when no drug molecules were present in the mixture (right). The images highlight the crucial role of the drug compounds for nanoparticle assembly. **C:** Mechanism of drug cargo cell uptake. The DNCs latch onto the cell surface through interaction with specific receptors (the SR-BI protein receptor). Interactions between the surface peptides of the DNCs enable delivery of the encapsulated drug cargo (red spheres) into the cell interior. Reprinted with permission from Zhang et al., *Angew. Chem. Int. Ed.* **48** (2009), 9171–9175, © 2009 John Wiley & Sons.

colleagues at the University of Toronto encapsulated a drug cargo within a phospholipid layer and added an amphipathic helical peptide to the vesicles which compacted and rigidified the resultant NPs. The NP surface-displayed helical peptide also contained a recognition sequence designed to dock onto specific cell-surface receptors and thus initiate cell uptake. The NP system depicted in Figure 5.6, denoted “drug nanocarrier” (DNC), represents a hybrid peptide/lipid/drug assembly in which the

“whole is greater than the sum of its parts”, providing a potentially versatile biological delivery platform.

*Lipoproteins* are a class of biomolecules which form nanoparticle aggregates in their natural environment – within the bloodstream. In fact, the critical function of capturing and transporting cholesterol and other lipids in blood vessels is accomplished via adsorption of the target lipids within naturally-assembled *lipoprotein NPs*. For example, the notorious *low-density lipoprotein (LDL)*, popularly known as the “bad cholesterol”) constitutes, as its name implies, NPs which are less compact compared to *high-density lipoprotein (HDL)*. Attempts have been made to “engineer” lipoprotein NPs with the aim of constructing biomimetic functional materials.

Figure 5.7 depicts a process in which natural LDL NPs were coupled with *gadolinium ions* (common contrast agents in magnetic resonance imaging) and used for imaging of *atherosclerotic plaques*, the pathological hallmarks of coronary heart disease.

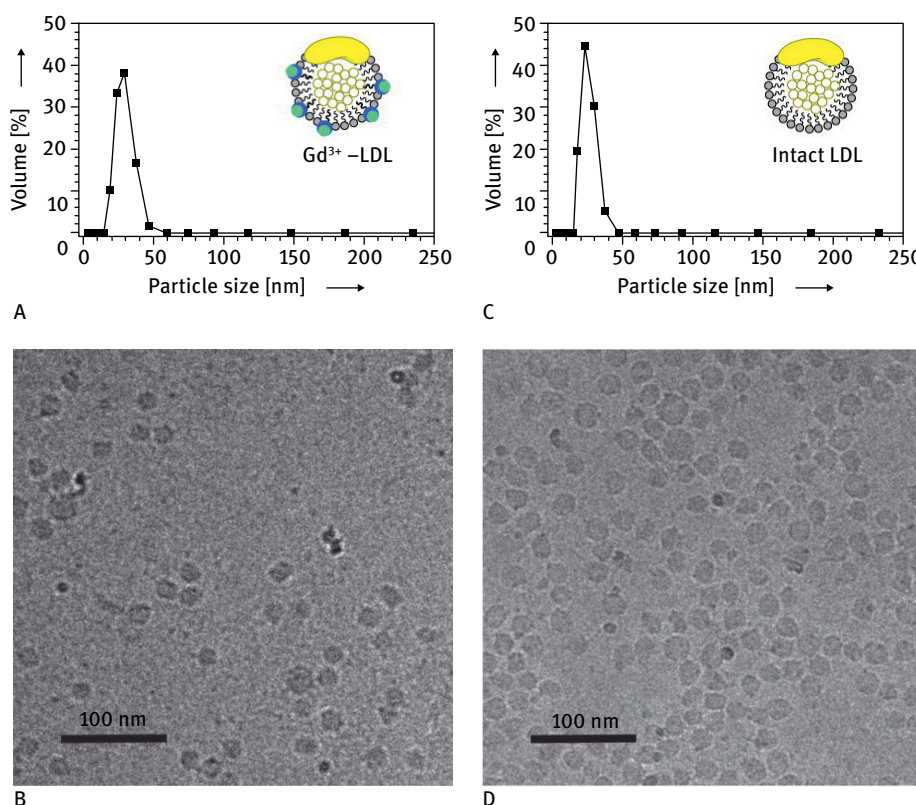


**Fig. 5.7:** Gadolinium-labeled low-density lipoprotein (LDL) nanoparticles. **A, B:**  $\text{Gd}^{3+}$ -labeling does not alter the size distribution of the LDL nanoparticles. **C, D:** Electron microscopy images further confirm that both nanoparticle species exhibit similar morphologies. Reprinted with permission from Lowell et al., *Bioconjugate Chem.* **23** (2012), 2313–2319, © 2012 American Chemical Society.

Conjugation of the  $\text{Gd}^{3+}$  ions to the LDL NPs was carried out by Y. Yamakoshi and colleagues at the University of Pennsylvania by incubating the nanoparticles with a lipid-like  $\text{Gd}^{3+}$  “chelating residue”. LDL NPs are known to deposit atherosclerotic plaques in blood vessels and contribute to their growth. As a consequence of the accumulation of the  $\text{Gd}^{3+}$ -labeled NPs, significant enhancement of MRI signals from atherosclerotic plaques was achieved in a mouse model by the researchers. The composite NPs in Figure 5.7 provide a vivid example of the multifunctionality and versatility inherent to lipoprotein-based NPs.

Peptide-based NPs might serve as vaccines. Generally, a vaccine comprises of the *immunogen* – substance recognized by the host which elicits an immune response – and *adjuvant*, a material enhancing immune action, for example through surface display and stabilization of the biologically-active conformation of the immunogen. NPs could fulfill these prerequisites since they constitute an effective platform for delivery and presentation of biological molecules on their surface. Figure 5.8 depicts an NP vaccine design in which two distinct proteins were linked together – *hemagglutinin (HA)*, functioning as the immunogen, and *ferritin*, a ubiquitous protein which assembles into compact NPs, serving as the delivery scaffold. HA is a prominent protein displayed on the surface of the *influenza* virus and is known to generate an immune response against the virus. In the system depicted in Figure 5.8, HA was fused to ferritin via genetic engineering, with the ferritin NPs stabilizing the bio-active conformation of HA extending from the NP surface. The composite ferritin-HA protein NPs were found by G. J. Nabel and colleagues at the National Institutes of Health, US, to elicit a broad immune response against the influenza virus.

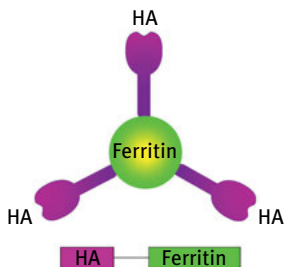


**Fig. 5.8:** Biological nanoparticle vaccine. Hemagglutinin (HA), an immune-triggering protein displayed on the surface of the influenza virus, was linked to ferritin, a protein forming compact nanoparticles. The HA units elicited an immune response when injected, indicating that HA adopted biologically-active conformation when attached to the ferritin nanoparticle.

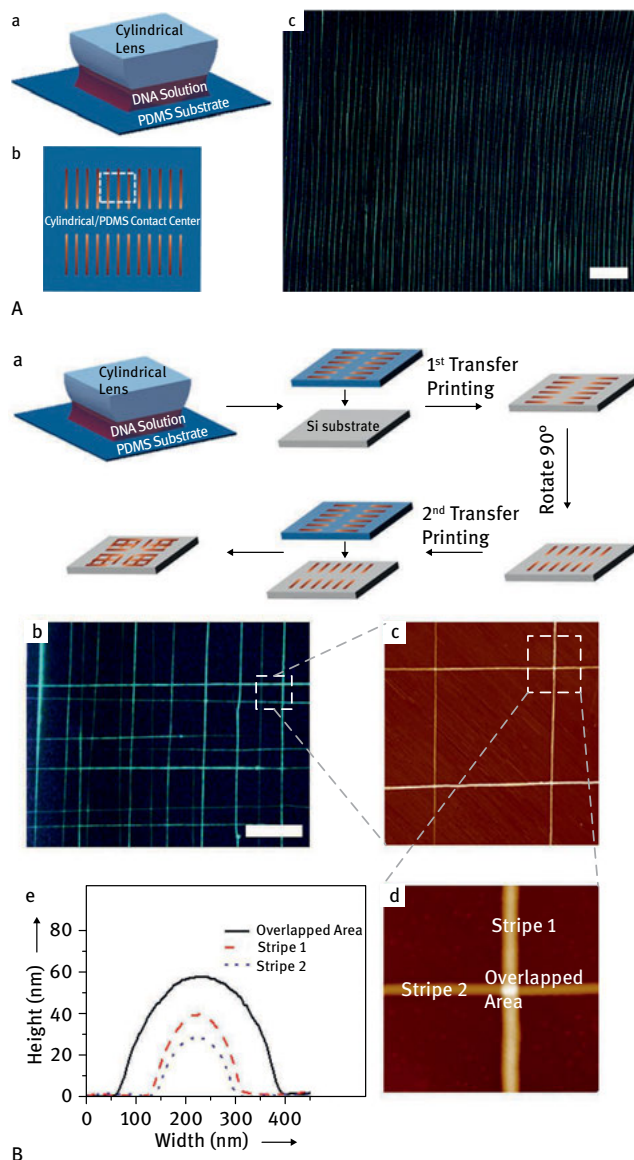
DNA is the fundamental information-bearing molecule in the cellular world. In the context of nanotechnology, the modular organization of DNA, i.e. base-pair complementarity underlying the double helix configuration, makes DNA a useful building block to construct a variety of structures, both in micro- and nanoscales. In particular, the elongated DNA strands are amenable to nanowire formation; *DNA-based nanowires* have been prepared via various routes. In aqueous solutions, however, DNA tends to adopt “coiled” conformations; accordingly efforts in this field have been directed to a large extent at “stretching” DNA NWs, usually by deposition on surfaces.

Figure 5.9 illustrates an elegant method for aligning DNA NWs on polymer surfaces. The phenomenon exploited by Z. Lin and colleagues at the Georgia Institute of Technology to create the oriented DNA assemblies is the accumulation and subsequent precipitation of DNA molecules at the edge of slowly evaporating water meniscus (conceptually similar to grains of sands deposited at the edges of receding waves on the beach). Accordingly, the researchers pressed a cylindrical lens upon a DNA solution placed on a flat polymer substrate. The interface between the curved cylinder and the flat surface created a confined geometry which reduced random solution flow and minimized instabilities, resulting in gradual deposition of oriented DNA NWs at the receding fronts of the evaporating aqueous solution. Intriguingly, the evaporative-alignment approach also enabled formation of *cross-shaped* nanowire structures via 90-degree rotation of the cylindrical lens (Fig. 5.9B).

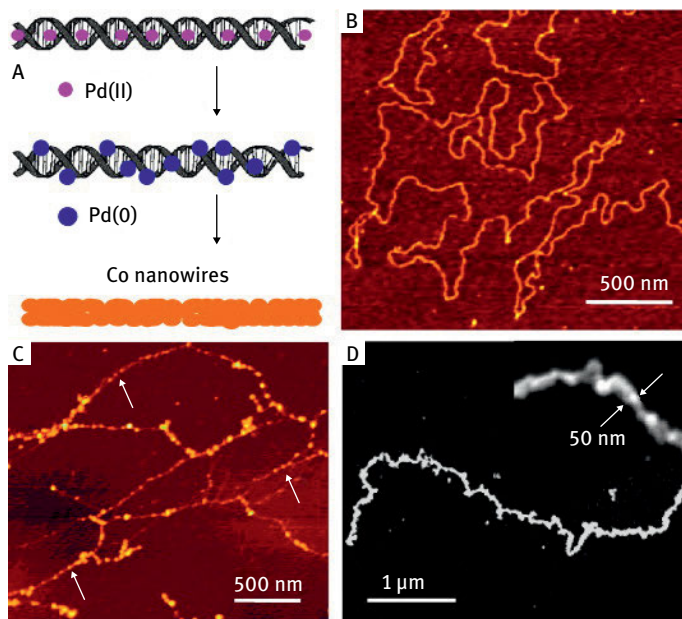
DNA NWs have often been used as templates in material design. This line of research is based on the versatile routes for chemical modification of oligonucleotides, allowing display of different functional units on DNA strands, such as thiols (for coupling with gold substances, for example in conducting electrodes), silanes (allowing conjugation with glass surfaces), amines, and more. Chemically speaking, one can perceive DNA molecules as programmable polymers whose structures can be modulated in the nanoscale by the intrinsic information-bearing features of oligonucleotide complementarity. Moreover, studies such as the one depicted above demonstrating DNA *ordering* (i.e. Fig. 5.9) indicate that DNA might serve as a useful template for metallic structures and devices.

Figure 5.10 depicts an experiment in which a DNA network was used as a scaffold for fabrication of metal nanowires. The experiment, designed by Q. Gu at Pacific Nanotechnology Inc., exploited the electrostatic attraction between the negatively-charged DNA and positive  $Pd^{2+}$  ions. The palladium ions bound to the DNA NW template were subsequently reduced to  $Pd^0$  particles, which in turn constituted nucleation sites for cobalt deposition, ultimately yielding continuous Co NWs. This generic approach was employed to create various metal nanowire arrays, pointing to potential use of DNA NWs in *nanoelectronics* applications.

DNA templates which are not “wire-like” (i.e. linear) have also been reported. Figure 5.11 highlights a simple method for assembling *circular* DNA rings and their use as templates for deposition of metallic silver. The experimental system designed by A. A. Zinchenko and colleagues at Kyoto University, Japan, exploited electrostatic attraction between negatively-charged DNA and a highly positively-charged *polycation*, resulting in the DNA folding into a compact “nanoring” structure. Subsequently, similar to the metal NW scheme discussed above (Fig. 5.10), positive  $Ag^+$  ions were embedded within the DNA template via binding to the negative DNA units. The  $Ag^+$  ions were then reduced, yielding “doughnut-shaped” metallic silver NPs. Notably, the silver nanorings gave rise to distinctive plasmon resonance light absorbance, pointing to possible use of the NP templating technique in optical modulation applications.



**Fig. 5.9:** Alignment of DNA nanowires. **A:** Alignment of DNA nanowires on a flat polymer surface achieved via slow evaporation of the DNA solution underneath a cylindrical "stamp". (a) Schematic diagram of the experiment and (b) the DNA nanowire array generated. The microscopy image in (c) shows a representative DNA nanowire array deposited on the surface, indicated by a broken line in (b). **B:** Production of a "crossed nanowire" array: (a) The experimental scheme, involving two consecutive alignment steps in which the cylindrical stamp is rotated by  $90^\circ$  between the two evaporation stages; (b-d) microscopy images depicting the perpendicular DNA nanowires; (e) a cross-section of the DNA nanowire intersection showing the overlapped area. Reprinted with permission from Li et al., *ACS Nano* 7 (2013), 4326–4333, © 2013 American Chemical Society.



**Fig. 5.10:** DNA as a template for metal nanowires. **A:** Schematic diagram of the nanowire deposition method. Palladium ions are electrostatically attracted to the DNA strand and subsequently reduced. The  $\text{Pd}^0$  metal seeds constitute nucleation sites for deposition of cobalt, producing metallic cobalt nanowire. **B:** Atomic force microscopy (AFM) image showing the DNA wire. **C:** AFM image of the DNA wire after reduction of the embedded palladium ions with apparent individual Pd nanoparticles. **D:** Scanning electron microscopy (SEM) image of the continuous cobalt nanowire; the inset shows a magnified view. Reprinted from *Mater. Lett.* Vol 62, Q. Gu and D. T. Haynie, *Palladium nanoparticle-controlled growth of magnetic cobalt nanowires on DNA templates*, pp. 3047–3050, © 2008, with permission from Elsevier.

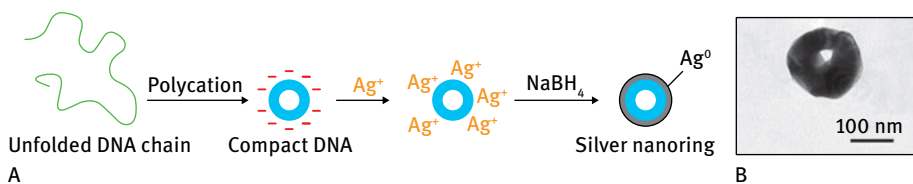


**Fig. 5.11:** Circular DNA as a template for silver deposition. **A:** Schematic diagram of the experiment: unfolded DNA chain is compacted into a “nanoring” structure via addition of polycations;  $\text{Ag}^+$  ions are attracted to the DNA template by electrostatic attraction; subsequent reduction yields “doughnut-shaped” silver nanorings. **B:** Electron microscopy image showing the Ag nanoring. Reprinted with permission from Zinchenko et al., *Adv. Mater.* **17** (2005), 2820–2825, © 2005 John Wiley & Sons.

Similar to DNA, *ribonucleic acid (RNA)* molecules exhibit base-pair complementarity (the nucleotide *thymine* in DNA is substituted in RNA sequences with *uracil*), enabling design of intriguing programmable nanoparticles. RNA, however, exhibits important differences to DNA which could render it particularly attractive for nanoparticle design applications. Since RNA usually occurs in single strands, rather than the double strand configurations abundant in DNA, it can adopt a variety of tertiary structures, including helices, loops, bulges, and stems, which could be employed as building blocks for diverse nanoparticle architectures. Examples of RNA-based nanoparticles are presented in Figure 5.12. These unique nanostructures were designed by L. Jaeger and colleagues at the University of California, Santa Barbara, using L-shaped RNA modules containing “reactive loops” and “stems” which assembled into distinct square-shaped nanoscale configurations. Uniform nanosquares exhibiting distinct dimensions were produced using different RNA motifs. Links between the RNA units forming the squares depended on the properties of the RNA building blocks, i.e. positioning of the reactive loops, size of the RNA “stems”, etc.

The design strategy for DNA and RNA nanoparticles is intimately linked to the intrinsic information-bearing properties of these two molecules. First, the structure of the desired nanoparticle and its functional objectives are defined. A computational scheme is then applied to determine the core DNA/RNA sequences. The building blocks are then generated via transcription of the long strand DNA/RNA, or by chemical synthesis of the smaller sequences. Ultimately the individual subunits are mixed and assembled into the NP architecture. This generic scheme can be augmented by attaching the oligonucleotide modules to other functional units, such as metallic species, fluorescent probes, and others, either in the assembly stage, or after producing the desired nanoparticle structures.

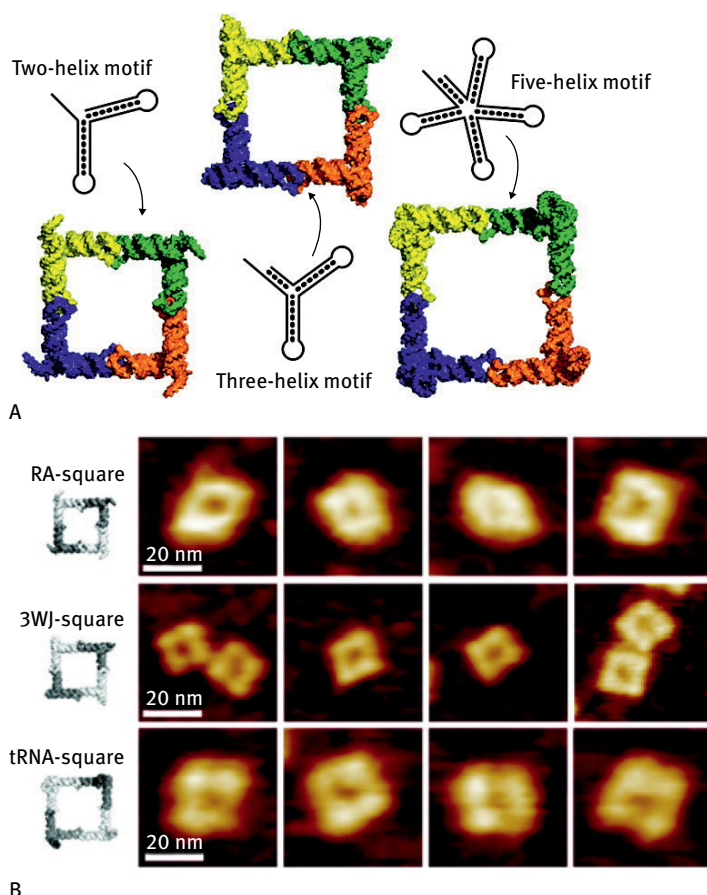


**Fig. 5.12:** RNA nanoparticles. **A:** Schematic drawing of three nanosquares assembled from distinct RNA motifs. The nanosquares comprise of L-shaped RNA modules (shown in different colors) which assemble by binding at the “stems”. The RNA motifs determine the properties of the L-shaped components and the assembled nanosquares. **B:** Atomic force microscopy (AFM) images of the nanosquares. The schematic structures corresponding to the different RNA modules are shown on the left. Reprinted with permission from Severcan et al., *Nano Lett.* **9** (2009), 1270–1277, © 2009 American Chemical Society.

## 5.2 Organic and polymeric nanoparticles

Organic chemistry, polymers in particular, has contributed its “fair share” to nanoparticle science and technology. Advanced synthetic capabilities make production of sophisticated nanoparticles from organic building blocks possible. Similar to the biological NPs discussed above, several organic NP systems have been found to exhibit interesting properties as independent entities, while in some instances organic NPs were used as templates for assembly of (usually metallic) NPs.

Various techniques have been introduced to prepare organic and polymeric NPs. *Laser ablation*, mostly applied for generation of metallic NPs, is one of the “top-down” strategies successfully employed to produce organic NPs in solution. This method is based on intense laser irradiation of organic microstructures (e.g. powders) suspended in water; the “chipped” NPs can subsequently be dispersed in water. “Bottom-up” techniques for the production of polymer NPs have also been introduced. Such schemes generally utilize *internal cross-linking* within the polymer chain, generating condensed nanoparticles. Figure 5.13 illustrates a prototypical reaction scheme for generating polymer NPs. The process, developed by G. W. Coates and colleagues at Cornell University, employed a polymer chain with distinctively-spaced pendant *vinyl* residues (shown in red in Fig. 5.13). Reaction between the vinyl units resulted in intra-molecular crosslinking which stabilized condensed NPs. Many variations of this generic synthetic approach have been reported, endowing diverse physical, chemical, and biological properties to polymer-based NPs.

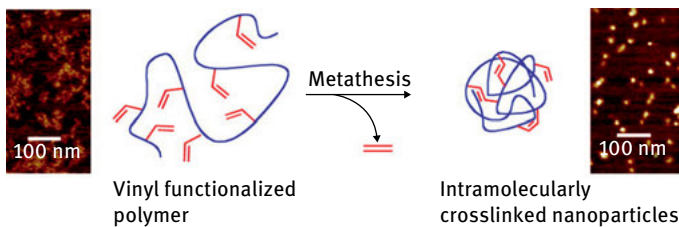


**Fig. 5.13:** Polymer nanoparticles assembled by internal crosslinking. Crosslinking is carried out through the pendant vinyl (i.e. ethylene) residues, shown in red. The atomic force microscopy (AFM) images depict the spread-out polymer chains (left) and the compact nanoparticles assembled by crosslinking (right). Reprinted with permission from Cherian et al., *JACS* **129** (2007), 11350–11351, © 2007 American Chemical Society.

*Polymer quantum dots* (or “Pdots”) are a fascinating class of NPs with potentially broad applications. Pdots are constructed from  $\pi$ -conjugated semiconducting polymers exhibiting direct bandgaps due to overlap of  $\pi$ -electron energy levels (Fig. 5.14). Such conjugated polymers can assemble into bright, fluorescently-tunable NPs on precipitation in various solvents; Pdots have also been prepared via direct reaction of the monomers in emulsions. Similar to the inorganic semiconducting quantum dots (Qdots) discussed in detail in Chapter 2, Pdots exhibit significant potential as bioimaging agents. Pdots, in fact, offer advantages for imaging since they feature extremely bright fluorescence, as the NPs consist of a high concentration of the luminescent semiconducting polymers compacted in a small volume. In addition, Pdots can quite easily be chemically-modified via well-developed polymer chemistry routes, making display of various functional units on their surface possible. Furthermore, polymeric building blocks are likely to be less toxic to cells than inorganic Qdots.

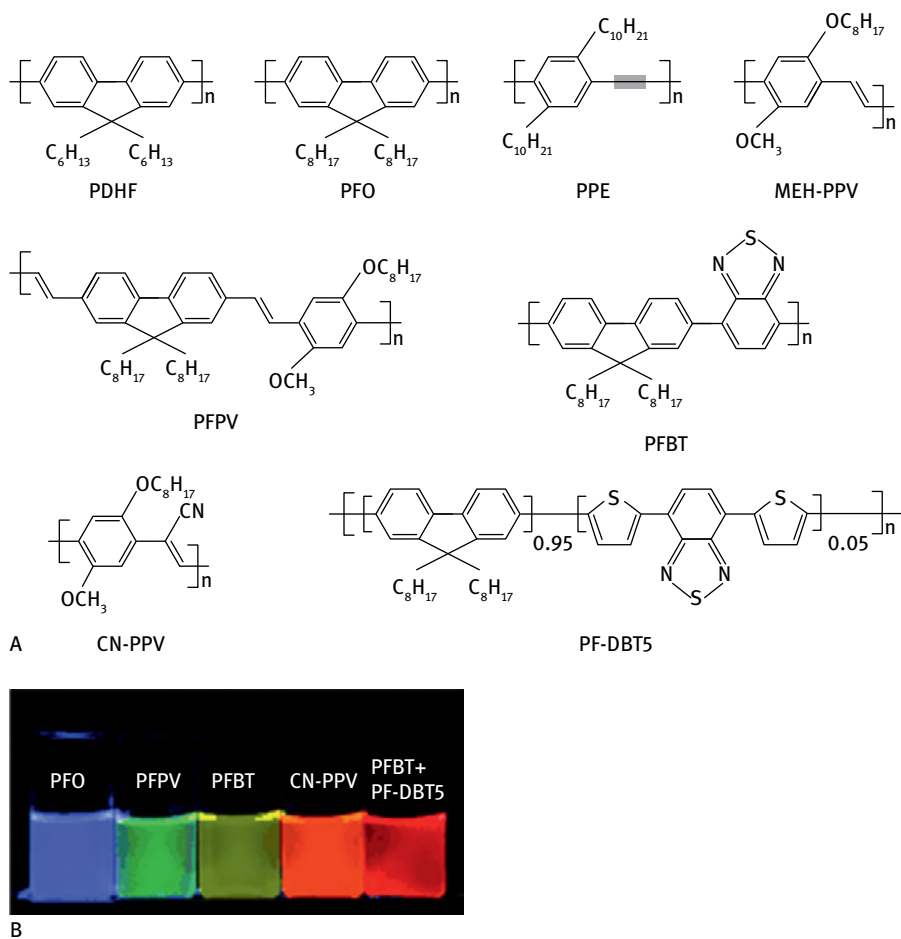


**Fig. 5.14:** Polymer quantum dots (Pdots). **A:** Conjugated semiconducting polymers used in construction of Pdots. **B:** Distinct colors (i.e. luminescence wavelengths) of Pdots comprising of different polymer materials. Reprinted with permission from Wu and Chu, *Angew. Chem. Int. Ed.* **52** (2013), 3086–3109, © 2013 John Wiley & Sons.

Pdots can be prepared either via condensation of the monomers followed by polymerization reactions, or (the more popular approach) by using the already-polymerized chains for assembly of the nanoparticles through crosslinking reactions. The latter technique is simpler for nonexperts to carry out, and obviates the use of specialized polymerization reagents which could interfere with biological applications of the NPs. Pdots have been produced from *hydrophilic*, *hydrophobic*, or *amphiphilic* polymer units, making these NPs a versatile platform. Furthermore, Pdots can contain other polymer (or biological) components in addition to the *luminescent* polymer

species, and the semiconducting polymers themselves can easily be coupled with other functional units.

Figure 5.15 depicts a representative biologically-functionalized Pdot system and its application in bioimaging. The functionalized Pdots, developed by D. T. Chiu and colleagues at the University of Washington, were prepared by mixing two polymers: a semiconducting conjugated polymer (PFBT) and a polymer (polystyrene derivative)

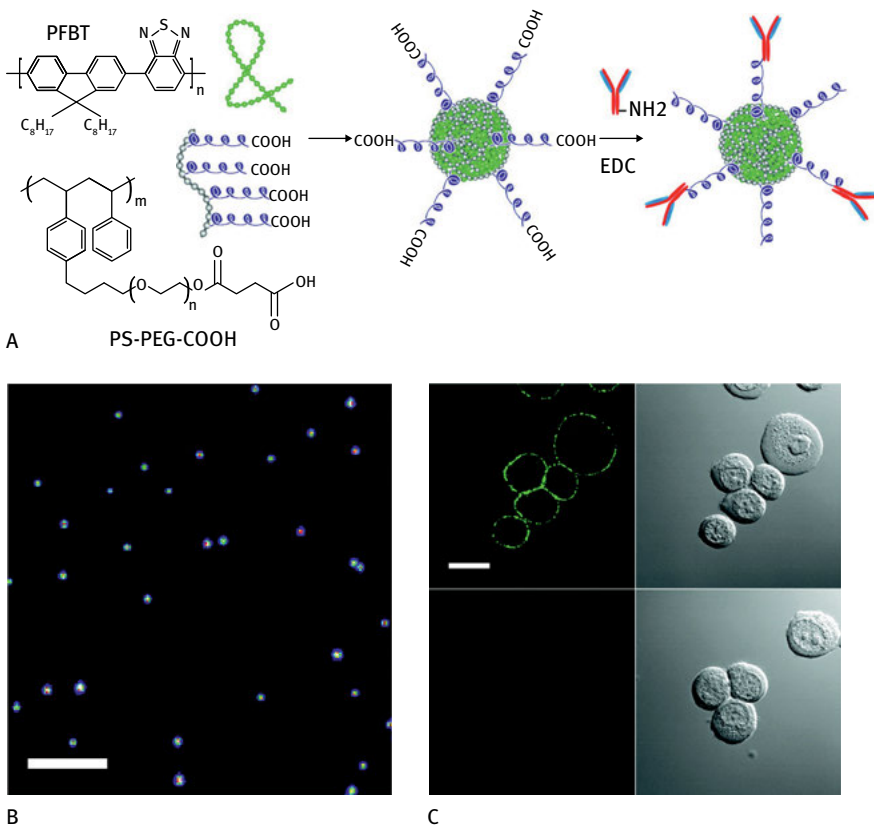


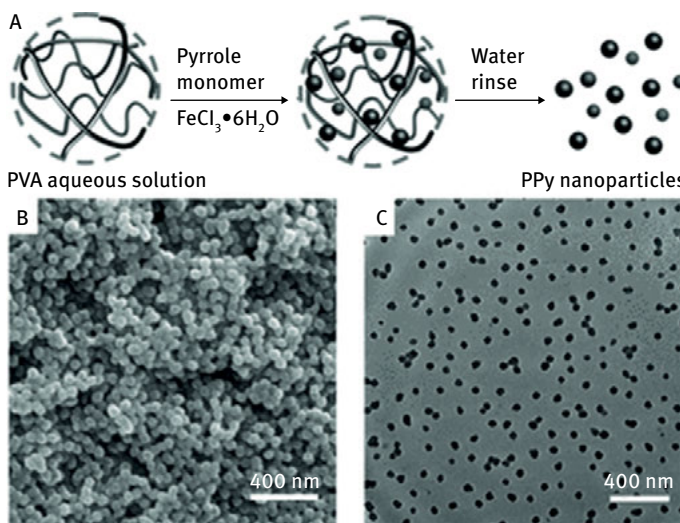
**Fig. 5.15:** Bio-conjugated polymer quantum dots (Pdots). **A:** Synthesis scheme: the Pdots are prepared by co-condensation of a semiconducting polymer (PFBT) and a polymer displaying carboxylic acid residues. The carboxylic residues are subsequently used for covalent coupling of antibody molecules (the “Y”-shaped residues). **B:** Single particle fluorescence microscopy depicting the bright Pdots. **C:** Cell imaging using the antibody-functionalized Pdots. The top left panel shows a fluorescence microscopy image of human breast cancer cells incubated with Pdots which were covalently-linked to antibodies recognizing a cell-surface receptor. No cell surface fluorescence was recorded when the cells were incubated with bare Pdots (not attached to antibodies, bottom panel). The panels on the right depict the bright field microscopy images indicating the cell positions. Reprinted with permission from Wu et al., *JACS* **132** (2010), 15410–15417, © 2010 American Chemical Society.

displaying abundant carboxylic moieties (Fig. 5.15A). The carboxylic units provided a facile chemical route for coupling the Pdots to biomolecules such as antibodies, which facilitated targeting of the particles to desired cellular locations. The single-particle fluorescence image in Figure 5.15B confirms the notable brightness of the Pdots; in fact, the fluorescence of the polymer NPs was notably more intense than many conventionally-used markers, such as organic fluorescent dyes or inorganic quantum dots. The high fluorescence and excellent photo-stability of the Pdots have made these NPs an excellent vehicle for cell imaging, highlighted in Figure 5.15C. The Pdots in the experiment were conjugated to antibodies directed against specific cell-surface receptors. The cell contours could be clearly deciphered when incubated with the Pdot-antibody constructs; no fluorescence was observed when bare Pdots (not coupled to the antibody) were used, confirming the occurrence of specific binding between the Pdot-antibody and the cell surface receptors.

While Pdots might serve as useful bioimaging agents, one should be aware of the limitations of their use, from both fundamental and technical points of view. Primarily, even though Pdots might exhibit minimal toxicity, they still constitute particles and as such, similar to conventional inorganic quantum dots, could have adverse effects when internalized within cells. It should also be emphasized that some semiconductor polymers do not easily adopt NP structures, while others exhibit broad fluorescence emission peaks, making them less attractive for bioimaging applications compared to inorganic quantum dots, which exhibit narrow emission spectra (and color tunability).

*Conductive polymers (CPs)* are another broad and important class of conjugated polymers for which the formation of nanostructures gives rise to interesting properties and applications. The “claim-to-fame” of CPs has been their excellent, metallic conductivity and their adoption of various morphologies and three-dimensional configurations. Nanoparticles of *polypyrrole (PPy)*, a well-known CP, have attracted interest in light of their *optical absorption* profile rather than electrical conductivity. Figure 5.16 depicts an experimental scheme developed by Z. Dai and colleagues at Harbin Institute of Technology, China, for production of spherical PPy NPs and their use as vehicles for photothermal therapy. Photothermal therapy is based on local heat dissipation from NPs following irradiation with near infrared (NIR) light, which penetrates tissues. Such applications have mostly been reported in the context of metallic NPs (see, for example, discussion on photothermal effects of Au nanorods in Chap. 3). In the system presented in Figure 5.16, PPy NPs were prepared inside a polymeric “cage”, serving as a stabilizing matrix. Importantly, the PPy NPs featured an absorbance peak at around 800 nm, well within the NIR spectral region. PPy NPs could be attractive for phototherapy applications as they should exhibit lower toxicity and greater long-term stability than Au and other metal NPs commonly studied as phototherapy platforms.

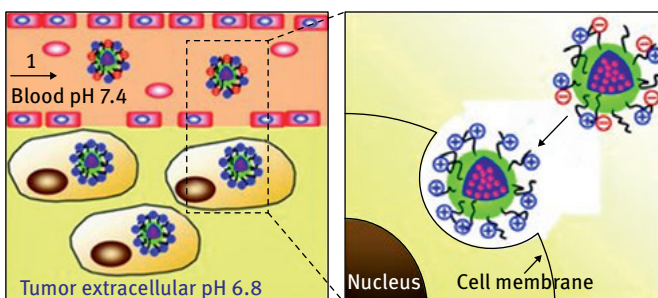
Similar to other nanoparticle systems, polymer NPs can be used as platforms for drug delivery. Contributing to such applications are synthetic methodologies developed to load therapeutic cargoes in polymer NPs, either by physical encapsulation (in



**Fig. 5.16:** Polypyrrole (PPy) nanoparticles. **A:** Synthesis scheme: pyrrole monomers embedded within a matrix of polyvinyl alcohol (PVA) acting as a stabilizer. Addition of the oxidizing agent ferric chloride ( $\text{FeCl}_3$ ) produces reaction centers for generation of the PPy nanoparticles. The PVA cages are finally dissolved in an aqueous solution. **B:** Electron microscopy image of the PVA “cages” acting as reaction chambers. **C:** Electron microscopy image of the PPy nanoparticles after PVA dissolution. Reprinted with permission from Zha et al., *Adv. Mater.* **25** (2013), 777–783, © 2013 John Wiley & Sons.

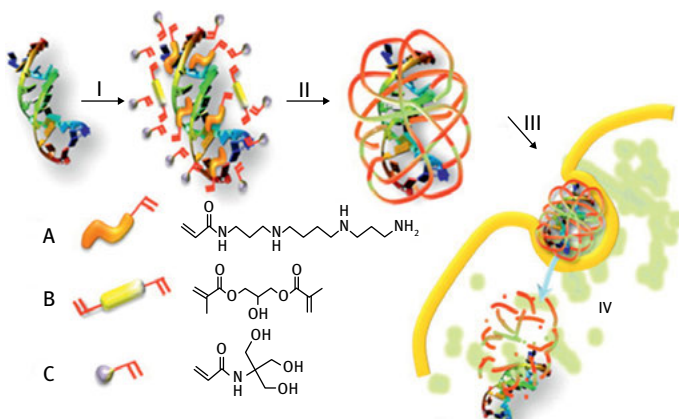
porous polymer NP host matrixes), or by covalent attachment to the polymer chains. Moreover, the diversity of polymeric substances used as nanoparticle building blocks provides a means for controlled release of the therapeutic cargo, for example by chemical cleavage or physical swelling.

Figure 5.17 presents a strategy for drug delivery to tumors using polymer NPs. The particles, designed by J. Wang and colleagues at the University of Science and Technology of China, comprised of a zwitterionic polymer (displaying both positive and negative charges) encapsulating doxorubicin, a commonly-used anti-tumor compound. The NPs retained their zwitterionic properties in circulating blood due to the neutral pH, and the corresponding neutral charge upon the particle surface made them relatively “inert” to cell uptake. However, in tumor environments the blood vessels become “leaky”, resulting in accumulation of NPs at the tumor site. Subsequently, since the micro-environment of cancer cells is highly acidic, the polymer surface became positive through an acid-promoted amide cleavage reaction. The positively-charged NPs were consequently attracted to the negatively-charged cell membrane and adsorbed by the cancer cells, releasing their therapeutic cargo (the doxorubicin molecules) inside the cells and destroying them.



**Fig. 5.17:** pH-based release mechanism of therapeutic cargo in polymer nanoparticles. The nanoparticles containing a therapeutic molecule are constructed from zwitterionic polymer chains. The nanoparticles retain their neutral charge in the physiological pH of 7.4 in blood. In tumor extracellular environments the acidic pH results in cleavage of the negative residues on the nanoparticle surface; the positively-charged polymer nanoparticles get adsorbed by the cancer cells, releasing their therapeutic cargo. Reprinted with permission from Yuan et al., *Adv. Mater.* **24** (2012), 5476–5480, © 2012 John Wiley & Sons.

Figure 5.18 presents another NP polymer-based delivery system – a “nanocapsule” designed to deliver small interfering ribonucleic acid (siRNA) into cells. siRNA is a promising therapeutic agent as its short RNA sequences bind to target RNA strands and consequently block expression of specific proteins. The challenge, however, is to deliver siRNA into the cell; the NPs depicted in Figure 5.18 accomplish this goal



**Fig. 5.18:** Polymer nanocapsules for siRNA delivery. The nanocapsule construction process comprises of enrichment of the RNA fragment with the monomers and crosslinkers (fragments denoted by **A**, **B**, **C**) used for (**I**) assembly of the nanocapsule; (**II**) polymerization to create the nanocapsule embedding the siRNA cargo; (**III**) cell uptake via endocytosis; and (**IV**) disintegration of the polymer capsule and release of the siRNA cargo. Reprinted with permission from Yan et al., *JACS* **134** (2012), 13542–13545, © 2012 American Chemical Society.

by encapsulating the siRNA sequence within a biodegradable polymeric matrix. The polymer layer has several functions – maintaining intactness of the siRNA cargo while transporting through the bloodstream, protecting against degradation by serum enzymes, and eventually inducing intracellular release through disintegration in the low pH environments of the “endosomes”, the cell compartments responsible for the uptake of extracellular particles.

While various polymer-based NPs for drug delivery feature particles prepared with the therapeutic cargo embedded within the polymer matrix comprising the nanoparticles, hollow NPs would have distinct advantages as they can be loaded with different molecular guests. Figure 5.19 depicts such hollow polymer NPs, prepared in different shapes and morphologies. Synthesis of the hollow NPs was carried out by simply drying micelle solutions of an amphiphilic block copolymer (polymer containing “blocks” of different monomer units). Rather surprisingly, R. K. O'Reilly and colleagues at the University of Warwick, UK, discovered that the drying conditions (specifically drying rate) had a profound effect on the NP morphology (spherical hollow NPs vs nanocylinders), internal topology, and volume. Importantly, the hollow

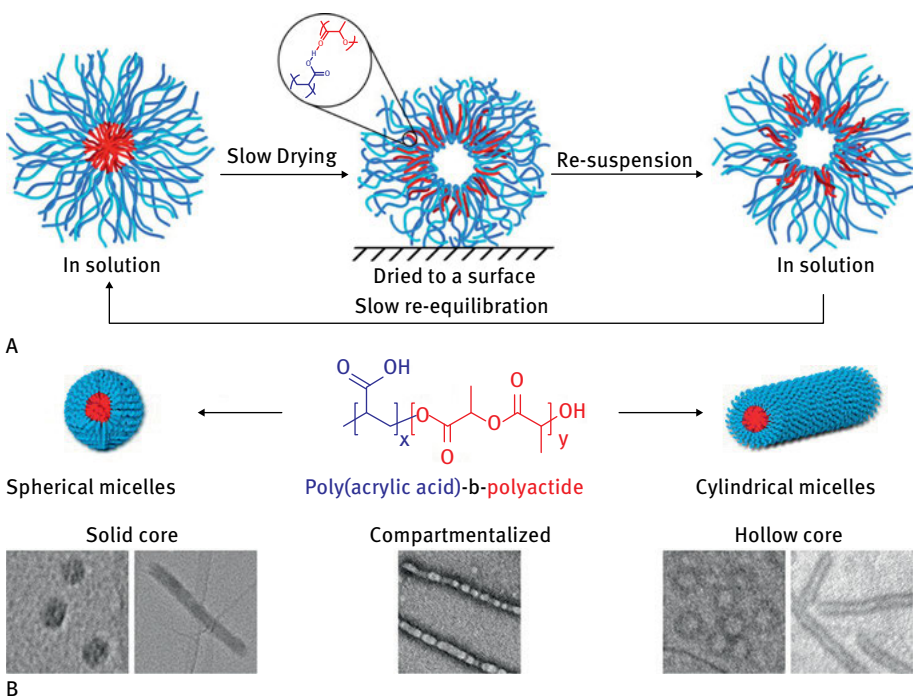


**Fig. 5.19:** Hollow polymer nanoparticles. **A:** Preparation of the hollow nanoparticles: upon slow drying, the polymer chains in the nanoparticle core rearrange and create a hollow space. **B:** Distinct polymer nanoparticle morphologies prepared. Reprinted with permission from Petzeltakis et al., *ACS Nano* 7 (2013), 1120–1128, © 2013 American Chemical Society.

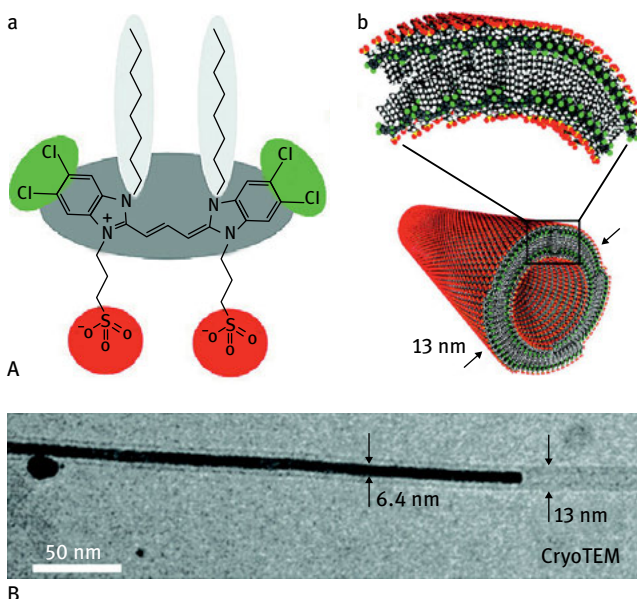


**Fig. 5.20:** Metal nanowire formation in cyanine nanotubular template. **A:** (a) Schematic diagram of nanotube assembly from cyanine; (b) the bilayer organization of the nanotube formed via interactions between the pendant hydrophobic sidechains of cyanine. **B:** Electron microscopy image depicting the Ag nanowire formed within the cyanine nanotube. Reprinted with permission from Eisele et al., *JACS* **132** (2014), 2104-2105, © 2013 American Chemical Society.

NPs could be re-suspended after drying and loaded with relatively high concentrations of molecular cargoes, pointing to their potential use in drug delivery.

Similar to the peptide-templated nanoparticles described above, organic molecules have also been used as scaffolds for deposition of metal NPs (Fig. 5.20). In an experiment carried out by J. P. Rabe and colleagues at Humboldt-Universitaet zu Berlin, Germany, an amphiphilic cyanine dye was used to construct a template for silver nanowires. The dye molecule played a dual role. One function was structural in nature – adopting an extended nanotubular structure via interactions between the pendant amphipathic carbohydrate sidechains (Fig. 5.20A), in which both the inner and outer surfaces were available for metal deposition. The other role of the cyanine molecules was to promote adsorption of silver ions by electrostatic attraction to the dye's negatively-charged phosphate residues. The bound  $\text{Ag}^+$  ions were subsequently reduced to metallic silver following light irradiation (i.e. “photo-initiated reduction”). Overall, the cyanine “superstructures” were shown to act as a combined chemical/physical platform for controlled deposition of uniform Ag nanowires.

